Convergence of phase fluctuation induced by intrachannel four-wave mixing in differential phase-shift keying transmission systems via phase fluctuation averaging

Chia Chien Wei and Jason (Jyehong) Chen

Institute of Electro-Optical Engineering and Department of Photonics, National Chiao-Tung University, 1001 Ta Hsueh Road, Hsin-Chu, Taiwan, 300

Received January 9, 2007; revised February 11, 2007; accepted February 12, 2007; posted February 16, 2007 (Doc. ID 78828); published April 17, 2007

This work investigates the effect of phase fluctuation averaging on phase fluctuation induced by intrachannel four-wave mixing (IFWM) in highly dispersed differential phase-shift keying transmission systems. Through repeatedly averaging the phase fluctuations of adjacent pulses, a simple analytical model and numerical simulation revealed that the IFWM-induced differential phase fluctuation is suppressed and convergent, even after an ultralong transmission. The influence of averaging the phase fluctuations on the bit error rate is also evaluated by the semianalytical method.

OCIS codes: 060.2330, 060.4370.

In recent years, the return-to-zero (RZ) differential phase-shift keying (DPSK) format has become a promising alternative to the traditional on–off keying format, especially for long-haul high-speed optical communication systems.[1] However, since DPSK signals are demodulated via a delay interferometer in front of a receiver, both amplitude fluctuation (AF) and phase fluctuation (PF) will degrade the performance of received signals, and the regeneration of the DPSK format should be able to reduce AF and/or PF to extend the transmission distance. Although a phase-sensitive amplifier could eliminate both AF and PF simultaneously, a complicated and impractical optical phase-locking pump beam is required.[2] Nevertheless, the AF of DPSK signals can be effectively eliminated by several phase-preserving amplitude regenerators.[3,4] Thus, in the amplitude-managed DPSK systems with these regenerators, accumulated PF is mainly responsible for the limit on the reach of signals. Moreover, with respect to dispersion-managed high-speed transmissions, the nonlinear phase noise generated from the beating between the amplified spontaneous emission (ASE) noise and the signal could be reduced through noise suppression[4] and pulse broadening.[5] Accordingly, the accumulated PF in amplitude-managed highly dispersed RZ DPSK systems is due mostly to the linear phase noise caused by the ASE noise and the nonlinear PF induced by intrachannel four-wave mixing (IFWM).

A novel phase noise averager (PNA) was recently proposed to average the PFs of two adjacent pulses,[6] and the differential PF (DPF) between neighboring bits converges even after an ultralong distance. However, the earlier work considered the PFs of neighboring bits to be uncorrelated.[6] For a high-bit-rate (>40 Gbits/s) system, since IFWM leads to partial correlation between the PFs of adjoining bits,[7] the effects of PNAs must be reexamined. Extending the previous work,[6] this Letter discusses the effect of PF averaging on IFWM-induced PF. Even though a correlation exists between the PFs, this work confirms that IFWM-induced DPF remains suppressed and convergent in DPSK transmission systems with periodically inserted PNAs. By estimating the bit-error rate (BER) with a semianalytical method, the effect of PF averaging is corroborated with the estimations of nonlinear penalties. To our best knowledge, the IFWM-induced PF is effectively eliminated for the first time.

Although the IFWM-induced PF is caused by the beating of broadened optical pulses under highly dispersive conditions, and therefore its strength is deterministic, it shows almost random statistics due to the random data of optical pulses.[7] However, the characteristics of IFWM-induced PF differ from those of ASE-related phase noise. First, if fiber spans including standard single-mode fiber (SSMF) and corresponding dispersion-compensating fiber (DCF) are employed repeatedly one after the another, the PFs generated in all spans are identical and add coherently span after span as the worst case.[8] Hence, while the variance of the PF caused in each span is σ^2, then the variance becomes $N^2\sigma^2$ after N spans, instead of $N\sigma^2$. Second, the PFs of adjacent bits are correlated, and this correlation is given by $\langle\varphi_m\varphi_n\rangle=\sigma^2C_{|m-n|}$, where $\langle\cdot\rangle$ denotes an expectation value; φ_n is the IFWM-induced PF of the nth bit in each span, and C_k is the correlation coefficient between the PFs of two pulses away from k bits. As a result, after N spans, the total DPF, $\Delta\Phi$, is $N(\varphi_n-\varphi_{n-1})$, and its variance is $\langle\Delta\Phi^2\rangle=2N^2\sigma^2(1-C_1)$.

Since a PNA can transform PF, φ_n, to become $\varphi_n^{(1)}=(\varphi_n+\varphi_{n-1})/2$, when the signals are sent through PNAs M times, the PF becomes $\varphi_n^{(M)}=2^{-M}\sum_{k=0}^{M}\binom{M}{k}\varphi_{n-k}$,[6] where $\binom{M}{k}$ is defined as $\Gamma(M+1)/[\Gamma(k+1)\Gamma(M-k+1)]$ and $\Gamma(\cdot)$ is the gamma function. Consequently, when a PNA is inserted behind every span, the total PF after N spans is $\Phi_n = \sum_{M=1}^{N} \varphi_n^{(M)} = \sum_{k=0}^{N} [\sum_{M=1}^{N} \binom{M}{k}/2^M] \varphi_{n-k}$. Note that this result is derived from the characteristics of the PF: φ_n are identical in all spans. Therefore the total DPF can be written as $\Delta\Phi = \Phi_n - \Phi_{n-1} = \sum_{k=0}^{N+1} a_k \varphi_{n-k}$, where the coefficients a_k are $\sum_{M=1}^{N} [\binom{M}{k} - \binom{M}{k-1}]/2^M = \delta_{0,k} + \delta_{1,k} - \binom{N+1}{k}/2^N$ and $\delta_{i,j}$ is the Kronecker delta function. Since φ_n are mutually correlated, the variance of the total DPF is not $(\sum_{k=0}^{N+1} a_k^2)\sigma^2$. This correlation is considered by writing the variance as

$$\langle \Delta\Phi^2 \rangle = \left(\sum_k C_k A_k \right) \sigma^2, \tag{1}$$

where A_k is the autocorrelation of a_k:

$$A_k = a_k \otimes a_{-k} = 2\delta_{0,k} + \delta_{1,k} + \delta_{-1,k} + 4\left[\frac{\begin{pmatrix} 2N+2 \\ N+k+1 \end{pmatrix}}{2^{2N+2}} - \frac{\begin{pmatrix} N+2 \\ k+1 \end{pmatrix}}{2^{N+2}} - \frac{\begin{pmatrix} N+2 \\ -k+1 \end{pmatrix}}{2^{N+2}} \right] \tag{2}$$

and $\otimes$ denotes convolution. The last three terms in Eq. (2) could be viewed as the binomial distributions, $P_p(k|Z) = \binom{z}{k} \times p^k (1-p)^{z-k}$ with $p=0.5$, centered at $k=0$, $N/2$, $-N/2$, with variances of $(N+1)/2$, $(N+2)/4$, and $(N+2)/4$, respectively. Then $\langle \Delta\Phi^2 \rangle$ is expected to approach a maximum value, when the first binomial distribution contributes the most to the product in Eq. (1), but the second and the third terms contribute little. Moreover, if two pulses are far from each other in the time domain, the correlation between their PFs should be zero. Consequently, as N is large, the main contribution to the DPF is $2\delta_{0,k} + \delta_{1,k} + \delta_{-1,k}$ in Eq. (2). That is, $\langle \Delta\Phi^2 \rangle$ converges to $2(1+C_1)\sigma^2$. However, the correlation coefficients are necessary to determine in detail the variation of the DPF with periodic PF averaging.

For simplicity to calculate C_k, the optical field of the nth pulse of RZ DPSK signals is assumed to be $u_n(t) = s_n \sqrt{P} \exp[-(t+nT)^2/(2\tau^2)]$, where $s_n = \pm 1$ indicates binary data encoded by a phase shift of either 0 or π; T is the bit period, and 1.66τ is the full width at half-maximum. Moreover, the nonlinear effect is treated as a perturbation to determine theoretically the distribution of the IFWM-indcued PF. However, in previous work,[7,8] nonlinearity in DCF was neglected. Actually, it significantly influences the characteristics of IFWM-induced PF, and especially the correlation between the PFs of neighboring bits. Accordingly, our analysis is extended to the nonlinear effects in both SSMF and DCF. From the previous work[7,8] and considering a complete postdispersion compensating scheme, the nonlinear PF can be represented as

$$\varphi_n = \sum_{l,m} s_l s_m s_n s_{l+m-n} [\gamma_1 P_1 F_{l,m}(L_1, \alpha_1, \beta_1'') - \gamma_2 P_2 e^{-\alpha_2 L_2} F_{l,m}(-L_2, \alpha_2, \beta_2'')], \tag{3}$$

where γ_i, P_i, L_i, α_i, and β_i'' are the nonlinear coefficients, the launch peak power, the length, the loss, and the group-velocity dispersion of SSMF ($i=1$) and DCF ($i=2$), and $F_{l,m}(L, \alpha, \beta'')$ is

$$F_{l,m}(L,\alpha,\beta'') = \Re \left[\int_0^L \frac{e^{-\alpha z}}{\sqrt{1 + 2j\beta'' z/\tau^2 + 3(\beta'' z/\tau^2)^2}} \times \exp\left\{ -\left(\frac{T}{\tau}\right)^2 \left[\frac{3lm}{1 + 3j\beta'' z/\tau^2} + \frac{(l-m)^2}{1 + 2j\beta'' z/\tau^2 + 3(\beta'' z/\tau^2)^2} \right] \right\} \mathrm{d}z \right], \tag{4}$$

giving the strength of the nonlinear effect from the lth, mth, and $(l+m)$th pulses. The first and second terms of Eq. (3) represent the nonlinear effects occurring in SSMF and DCF, respectively. Throughout this Letter, 40 Gbit/s RZ DPSK signals with a 33% duty cycle are considered; the length of SSMF in each span is 80 km; the nonlinear coefficients, the loss, and the group-velocity dispersion of SSMF and DCF are 1.3 and $5.4\ \mathrm{W^{-1}\,km^{-1}}$, 0.2 and 0.65 dB/km, and −21.7 and $127.6\ \mathrm{ps^2/km}$, respectively; the launch power of DCF is 7 dB lower than that of SSMF, and this power is chosen by setting the mean nonlinear phase shift $\Theta_{\mathrm{nl}} = N\gamma_1 P_{1,\mathrm{ave}} L_{1,\mathrm{eff}} + N\gamma_2 P_{2,\mathrm{ave}} L_{2,\mathrm{eff}}$ to a specific value, where $L_{i,\mathrm{eff}}$ is the effective length per span and $P_{i,\mathrm{ave}} = \sqrt{\pi} P_i \tau / T$ is the average launch power. Since the pulses are highly broadened when sent into DCF, two pulses will interact even though these pulses are far away from each other. Hence, all distributions of $-22 \leqslant l, m, l+m \leqslant 22$ in Eq. (3) are considered to fully capture pulse-to-pulse interactions, and $l \neq n$ and $m \neq n$ are set to exclude self- and intrachannel cross-phase modulation effects. With a De Bruijn sequence of 2^{16} bits and $\Theta_{\mathrm{nl}} = 1$ rad after 40 spans, Fig. 1 plots the correlation coefficients of PFs contributed to by both SSMF and DCF, SSMF only, and DCF only, and the corresponding distributions of φ_n and φ_{n-1} caused in each span are shown in insets. These figures clearly show that the nonlinear effect in DCF cannot

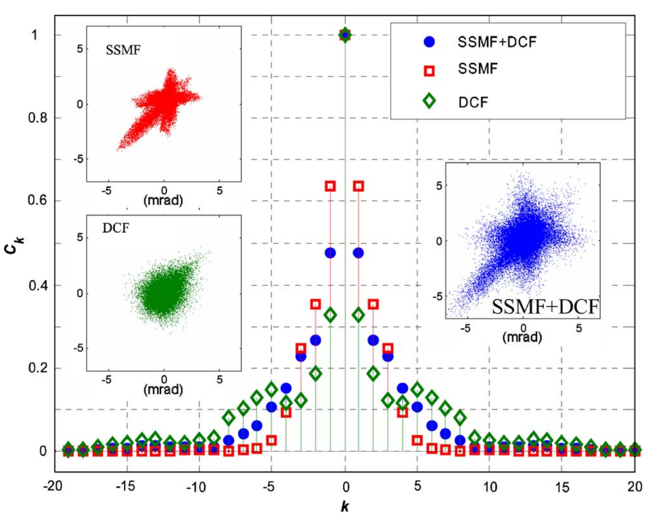

Fig. 1. (Color online) Correlation coefficients of the IFWM-induced PFs. Insets, corresponding distributions of φ_n and φ_{n-1}.

be neglected, and it increases the correlation of PFs of remote bits but decreases that of adjoining bits.

Based on the results of Fig. 1 and Eq. (1), Fig. 2 analytically plots the variance of DPF as a function of the number of the spans. The variance is maximal near 20 spans and converges to about $3\sigma^2$ very slowly. Figure 2 also plots the results of a numerical simulation using commercially available software to verify the effect of PF averaging. All of the parameters of the simulation are identical to those in Fig. 1, and ASE noise is neglected to focus on the pattern effects. When the number of spans is smaller than 20, the theory agrees excellently with the simulation. Since the amplitude of the signals is not regenerated in the simulation, the IFWM-induced AF generates additional nonlinear PF increasingly. Therefore, for $N>35$, $\langle\Delta\Phi^2\rangle$ with PNAs begins to increase rather than decrease. However, if ideal phase-preserving amplitude regenerators are inserted behind each span, then the simulation results will be identical to the theoretical results. Furthermore, both results without PNA in Fig. 2 agree that $\langle\Delta\Phi^2\rangle$ increases as the square of the distance.

To further investigate the improvement by PF averaging, a semianalytical method is used to compute the BER and the nonlinear penalties. The BER related to a signal-to-noise ratio (SNR), ρ_s, and the nonlinear DPF is equal to[8,9]

$$p_e = \left\langle Q_1\left(\sqrt{2\rho_s}\left|\sin\frac{\Delta\Phi}{2}\right|, \sqrt{2\rho_s}\left|\cos\frac{\Delta\Phi}{2}\right|\right) - \frac{e^{-\rho_s}}{2} \times I_0(\rho_s|\sin\Delta\Phi|)\right\rangle, \quad (5)$$

where $Q_1(\cdot,\cdot)$ is the Marcum Q function and $I_0(\cdot)$ is the modified Bessel function of the first kind. The BER curves as functions of the SNR with the IFWM-induced PFs are calculated based on Eqs. (3)–(5), and the conditions of $\Theta_{\rm nl}=1,3,5$ rad after 40 spans with and without PNAs are both plotted in Fig. 3. For comparison, the baseline shown in Fig. 3 is the BER without the PFs of $e^{-\rho_s}/2$. Note that all the BER curves with periodic PF averaging overlap the baseline, and this fact indicates that the nonlinear penalty is negligible. Moreover, both increasing the transmission distance and the launch power will increase and therefore degrade DPSK signals increasingly. In addition, longer sequences (up to 2^{24}) are tested in calculating both C_k and the BER, and the results do not change significantly with the length of the pulse train as it exceeds 2^{16}.

This work demonstrates that periodically inserting PNAs into RZ DPSK transmission systems can effectively suppress IFWM-induced PF. A comprehensive theoretical model that incorporates the nonlinear effect of DCF is established, and the results indicate that the PF induced in DCF cannot be neglected. A strong agreement between theoretical analysis and numerical simulation is shown, confirming the convergence of IFWM-induced PF with periodic PF averaging. Further, the semianalytical method is used to compute BER and shows that PF averaging can obviate nonlinear penalties.

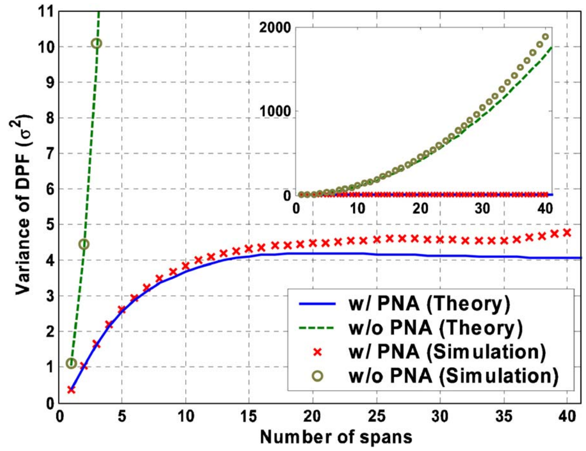

Fig. 2. (Color online) Variance of DPF as a function of the number of spans.

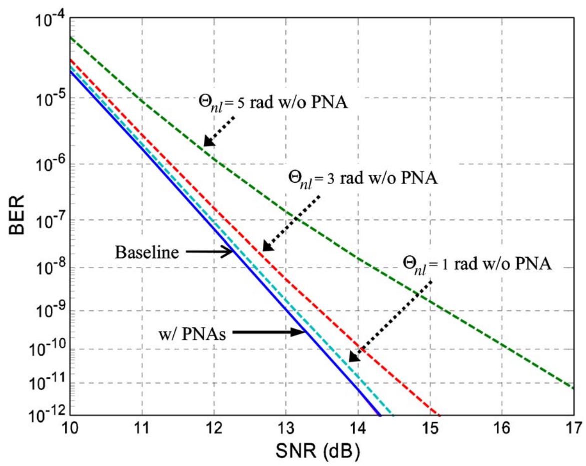

Fig. 3. (Color online) BER curves as functions of the SNR.

The authors thank the reviewers for valuable comments. This research was sponsored by the National Science Council, Republic of China, grants NSC 96-2752-E-009-004-PAE, 95-2221-E-009-225 and 95-2221-E-009-349. C. C. Wei's e-mail address is mgyso.wei@gmail.com.

References

1. C. Xu, X. Liu, and X. Wei, IEEE J. Sel. Top. Quantum Electron. **10**, 281 (2004).
2. K. Croussore, C. Kim, and G. Li, Opt. Lett. **29**, 2357 (2004).
3. A. G. Striegler, M. Meissner, K. Cvecek, K. Sponsel, G. Leuchs, and B. Schmauss, IEEE Photon. Technol. Lett. **17**, 639 (2005).
4. M. Matsumoto, J. Lightwave Technol. **23**, 2696 (2005).
5. X. Liu, C. Xu, and X. Wei, in *28th European Conference on Optical Communication, 2002, ECOC 2002* (IEEE, 2002), paper 9.6.5.
6. C. C. Wei and J. Chen, Opt. Express **14**, 9584 (2006).
7. X. Wei and X. Liu, Opt. Lett. **28**, 2300 (2003).
8. K.-P. Ho, IEEE Photon. Technol. Lett. **17**, 789 (2005).
9. K.-P. Ho, IEEE Photon. Technol. Lett. **16**, 308 (2004).